Opa1 Deficiency Leads to Diminished Mitochondrial Bioenergetics With Compensatory Increased Mitochondrial Motility

Shanshan Sun,[1] Irina Erchova,[1] Frank Sengpiel,[3,4] and Marcela Votruba[1,2]

[1]School of Optometry and Vision Sciences, Cardiff University, Cardiff, United Kingdom
[2]Cardiff Eye Unit, University Hospital of Wales, Cardiff, United Kingdom
[3]School of Biosciences, Cardiff University, Cardiff, United Kingdom
[4]Neuroscience & Mental Health Research Institute, Cardiff University, Cardiff, United Kingdom

Correspondence: Marcela Votruba, School of Optometry and Vision Sciences, Maindy Road, Cardiff University, Cardiff, CF24 4HQ, United Kingdom; votrubam@cardiff.ac.uk.

Received: March 3, 2020
Accepted: May 20, 2020
Published: June 19, 2020

Citation: Sun S, Erchova I, Sengpiel F, Votruba M. Opa1 deficiency leads to diminished mitochondrial bioenergetics with compensatory increased mitochondrial motility. *Invest Ophthalmol Vis Sci.* 2020;61(6):42. https://doi.org/10.1167/iovs.61.6.42

Purpose. Retinal ganglion cells (RGCs) are susceptible to mitochondrial deficits and also the major cell type affected in patients with mutations in the OPA1 gene in autosomal dominant optic atrophy (ADOA). Here, we characterized mitochondria in RGCs in vitro from a heterozygous B6; C3-*Opa1*^{Q285STOP} (*Opa1*$^{+/-}$) mouse model to investigate mitochondrial changes underlying the pathology in ADOA.

Methods. Mouse RGCs were purified from wild-type and *Opa1*$^{+/-}$ mouse retina by two-step immunopanning. The mitochondria in neurites of RGCs were labeled with Mito-Tracker Red for structure and motility measurement by time-lapse imaging. Mitochondrial bioenergetics were determined by the real-time measurement of oxygen consumption rate using a Seahorse XF^{e} 96 Extracellular Flux Analyzer.

Results. We observed a significant decrease in mitochondrial length in *Opa1*$^{+/-}$ RGCs with a remarkably higher proportion and density of motile mitochondria along the neurites. We also observed an increased transport velocity with a higher number of contacts between mitochondria in *Opa1*$^{+/-}$ RGC neurites. The oxygen consumption assays showed a severe impairment in basal respiration, Adenosine triphosphate-linked (ATP-linked) oxygen consumption, as well as reserve respiratory capacity, in RGCs from *Opa1*$^{+/-}$ mouse retina.

Conclusions. Opa1 deficiency leads to significant fragmentation of mitochondrial morphology, activation of mitochondrial motility and impaired respiratory function in RGCs from the B6; C3-*Opa1*^{Q285STOP} mouse model. This highlights the significant alterations in the intricate interplay between mitochondrial morphology, motility, and energy production in RGCs with Opa1 deficiency long before the onset of clinical symptoms of the pathology.

Keywords: autosomal dominant optic atrophy, retinal ganglion cells, OPA1, mitochondrial motility, mitochondrial bioenergetics

Autosomal dominant optic atrophy (ADOA) is one of the most common autosomal inherited optic neuropathies. It is characterized by a bilateral degeneration of the optic nerves, causing a slowly progressive, insidious visual loss, often beginning in childhood. There is irreversible pallor of the optic disc, reduced thickness of the nerve fiber layer and a ceco-central scotoma. The deficits are accompanied by a tritanopic dyschromatopsia.[1,2]

The nuclear optic atrophy 1 gene (*OPA1*) is responsible for most (75%), cases of ADOA.[3] Over 250 *OPA1* mutations have been reported in patients and a reduction in the amount of OPA1 protein (haploinsufficiency) is believed to be the major pathogenic mechanism in many ADOA cases.[4,5] OPA1 is ubiquitously expressed and plays a crucial role in the fusion process of inner mitochondrial membranes and in the maintenance of the normal architecture of mitochondrial cristae.[3,6] It is also involved in the maintenance of oxidative phosphorylation and membrane potential, as well as the control of apoptosis through anchoring cytochrome c. However, the cellular changes specific to retinal ganglion cell (RGC), the predominant cell type affected in ADOA,[7,8] caused by OPA1 deficiency before the onset of pathology and their mechanisms remain unclear. Thus we hypothesize that the alterations in mitochondrial dynamics during early asymptomatic stages of ADOA precede the neurodegeneration and consequent RGC cell death.

In our study, a heterozygous *Opa1* mutant mouse model (B6; C3-*Opa1*^{Q285STOP}) was used to model the pathophysiology of ADOA disease in mice, which carry a protein-truncating nonsense mutation in exon 8 immediately before

the central dynamin-GTPase, leading to a ~50% reduction in Opa1 transcript and protein in retina and neural tissues.[9] Here we provide a novel insight into the early changes in the morphology, motility, and bioenergetics of mitochondria in RGCs in early ADOA.

Materials and Methods

Mouse Breeding

The heterozygous *Opa1* mutation B6; C3-*Opa1*^{Q285STOP} was generated as previously described.[9] The founder generation mice were outcrossed to C57BL/6J (Charles River, UK) and the experiments were performed on the mice bred from generation 8 to 9. Mice were genotyped by *Opa1* allele-specific polymerase chain reaction.[9] All animal procedures were performed under license in accordance with the UK Home Office Animals Scientific Procedures (Animals) Act (1986) and the ARVO Statement for the Use of Animals in Ophthalmic and Vision Research. The Cardiff University Biological Standards Committee approved the experimental protocols. We followed the guidelines of the Animal and Plant Health Agency for compliance with Regulation (EC) 1069/2009 and implementing Regulation (EC) 142/2011 for the transport, storage, use, and disposal of animal by-products.

RGC Culture

All procedures for RGCs culture were carried out on six- to seven-day-old *Opa1*$^{+/-}$ and WT mouse pups using a two-step immunopanning protocol from Winzeler and Wang[10] with minor modifications. Briefly, the retina was dissected out from the mouse eye and dissociated and triturated into cell suspension. Afterward, cells were purified by two negative panning plates coated with Lectin from Bandeiraea simplicifolia (BSL-1; Vector Laboratories Ltd., United Kingdom) to remove the contaminating cell types and RGCs were finally selected by one positive panning plate coated with Thy1.2 (CD90) IgM (Serotec MCA02R, Bio-Rad Laboratories, Inc.) for 45 minutes at room temperature (25°C).

RGCs were collected and then seeded on glass coverslips (Academy Science Limited, UK) coated by Poly-D-lysine (Sigma-Aldrich Corp., St. Louis, MO, USA) and laminin (R&D Systems, Minneapolis, MN, USA) with a seeding density of 50,000 RGCs per well in 24-well culture plates (Nunc; Thermofisher, Waltham, MA, USA). RGCs were cultured in a humidified atmosphere at 37°C under 10% CO_2, in serum-free growth medium as previously described.[10]

The two-step immunopanning method can yield RGCs with high purity (>80%) from rodents in published research.[11–14] In our lab, the purity of cultured RGCs was identified by co-staining of anti-Thy 1.2 antibody and anti-RBPMS antibody (Abcam).

Mitochondrial Morphology Assessment

Totally 65 WT mouse pups and 60 *Opa1*$^{+/-}$ mouse pups were used for the three independent experiments. Purified RGCs were extracted from approximately 20 WT or *Opa1*$^{+/-}$ mouse pups in each panning procedure, plated in 24-well plates in three replicates and then stained by the specific mitochondrial marker, MitoTracker Red CMXRos (Molecular Probes, Invitrogen) at 37°C for 30 min on the eighth day in vitro. Images were captured under a oil magnification lens at ×63 using Zeiss LSM 880 confocal microscope and Zen Zeiss software (Carl Zeiss, Oberkochen, Germany). The length of each mitochondrial fragment was measured for morphological assessment by FIJI software (v1.52p, Wayne Rasband, National Institutes of Health, Bethesda, MD, USA).

Measurement and Classification of Mitochondrial Motility

Time-lapse imaging was used to record mitochondrial movements; images were captured every five seconds for 10 minutes from RGCs cultured from WT and *Opa1*$^{+/-}$ mouse pups (n = 20 to 25 for each group) in three replicates on the eighth day in vitro. Three independent experiments were performed. Kymographs of mitochondrial movements were generated by KymoAnlyzer[15] plugin in FIJI software.

Depending on the kymographs generated from the 10-minute mitochondrial movement recordings, the mitochondria were classified as stationary (that moved no further than 5 µm), or motile (moved further than 5 µm). The density of mitochondria was calculated as the number of stationary or motile mitochondria per length of the neurite in µm. The contact rate was calculated as the number of contacts between mitochondrial tracks divided by the total number of mitochondria per minute in each imaged region. The velocities of movements were calculated for motile mitochondria from the generated kymographs: the length of horizontal axis (the distance of movement) was divided by the length of vertical axis (the time of movement lasted) (µm/s).

Measurement of Mitochondrial Bioenergetics

The real-time measurement of oxygen consumption rate (OCR) was carried out by the Seahorse XF^e 96 Extracellular Flux Analyzer (Agilent Technologies, Santa Clara, CA, USA) using Seahorse XF Cell Mito Stress Test Kit (no. 103015-100, Agilent Technologies) according to the manufacturer's protocol. Briefly, cells were plated at the concentration of 20,000 cells/well in XF^e 96 microplates (Agilent Technologies) coated with Cell-Tak (no. 354240; Corning, Corning, NY, USA). OCR was measured in Seahorse XF DMEM Medium containing 10 mmol/L glucose, 1 mmol/L pyruvate, and 2 mmol/L l-glutamine (no. 103575-100, no. 103577-100, no. 103578-100, no. 103579-100, Agilent Technologies) under basal conditions and in response to three serial injected compounds—oligomycin (1.0 µmol/L), carbonylcyanide-4-(trifluoro- methoxy) phenylhydrazone (FCCP; 2.5 µmol/L), and a mixture of rotenone and antimycin A (1.0 µmol/L) to determine the values for the basal mitochondrial respiration, Adenosine triphosphate-linked (ATP-linked) oxygen consumption rate, maximal respiration, and spare respiratory capacity. Each sample was plated in five replicates. After the assays, the cells were immediately fixed and stained with Hoechest 33342, and then the images of whole well were captured by IX71 inverted microscope (Olympus, Tokyo, Japan) to calculate the number of cells in each well using FIJI software (v1.52p, Wayne Rasband, National Institutes of Health). OCR values were normalized to cell number. Three independent experiments were performed.

Investigative Ophthalmology & Visual Science

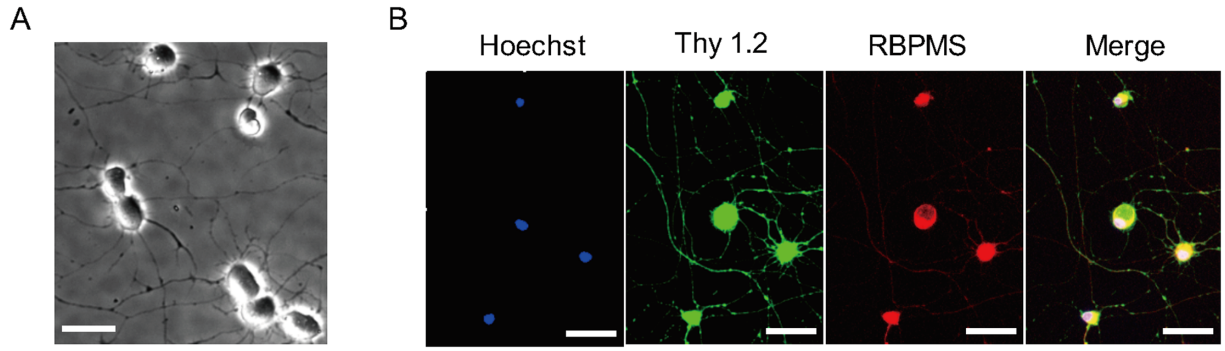

Figure 1. Identification of RGCs isolated by two-step immunopanning after two days in culture. (**A**) Phase-contrast image showing the characteristic morphology of RGCs. (**B**) Immunofluorescent staining with Hoechst 33342 (*blue*), Thy1.2 (*green*), RBPMS (*red*), and the merged image. Scale bar = 50 µm.

Statistical Analysis

The data are presented as means ± SEM. The data were normally distributed and compared statistically with unpaired Student's *t*-test using GraphPad Prism 8.0 (GraphPad, San Diego, CA, USA). A value of $P < 0.05$ was defined as statistically significant.

Results

Identification of Cultured RGCs

Approximately 23,000 to 27,000 RGCs were isolated from each mouse retina by two-step immunopanning. After two days in culture, RGCs were identified by their plump rounded cell bodies with characteristic long neurites (Fig. 1A). Cell identity was also verified histologically by immunofluorescent co-staining of Thy1.2 and RBPMS (Fig. 1B). The purity was approximately 85.22%, calculated as the ratio of double-stained Thy1.2 and RBPMS-positive cells to the total number of cells within imaged regions from five independent experiments.

Opa1 Deficiency Leads to Fragmented Mitochondrial Morphology in Primary Mouse RGCs

We measured the length of each mitochondrion along the RGC neurites and documented the distribution of mitochondrial length in µm using high-resolution confocal microscopy (See Fig. 2A). The length of mitochondria was 3.45 ± 0.20 µm in wild-type RGCs, whereas it was 1.92 ± 0.10 µm in *Opa1*$^{+/-}$ RGCs (decreased by 1.53 µm, $P < 0.01$, see Fig. 2B). Specifically, a significantly higher proportion of mitochondria with length < 1 µm (increased by ~16.19%, $P < 0.05$), as well as that of mitochondria with length between 1 and 2 µm (increased by ~30.71%, $P < 0.01$) were observed in *Opa1*$^{+/-}$ compared with the wild-type. However, there was an obviously smaller proportion of mitochondria with length between 3 and 4 µm (decreased by ~21.64%, $P < 0.01$), as well as that of mitochondria with length longer than 4 µm (decreased by ~18.26%, $P < 0.05$, see Fig. 2C). These results show a concentrated distribution of mitochondrial length in 3 to 4 µm in the wild-type RGCs, whereas it is 1 to 2 µm in *Opa1*$^{+/-}$ RGCs, indicating the fragmentation of mitochondria, often caused by Opa1 deficiency.

Opa1 Deficiency Activates Mitochondrial Motility in Primary Mouse RGCs

To investigate how Opa1 deficiency influences the mitochondrial movement within neurites of RGCs from wild-type and *Opa1*$^{+/-}$ mice, time-lapse imaging of live mitochondrial activity was performed. In total, 1280 mitochondria within 91 neurites from wild-type RGCs and 1205 mitochondria within 92 neurites from *Opa1*$^{+/-}$ RGCs were measured from three independent experiments. As shown in Figure 3A, the movement of each mitochondrion has been manually tracked in kymographs generated from the 10-minute time-lapse imaging.

In wild-type RGCs, 87.58% of mitochondria were stationary, and 12.42% of mitochondria moved further than 5 µm and were thus identified as motile. The distribution of the mitochondrial population showed that there was a significant increase in the proportion of motile mitochondria in *Opa1*$^{+/-}$ RGCs compared with that in wild-type RGCs (motile mitochondria increased by 10.53%, $P < 0.05$, see Fig. 3B). Consistently, the density of motile mitochondria per length of neurite in µm showed a marked increase in *Opa1*$^{+/-}$ RGCs compared with the wild-type ($P < 0.01$, see Fig. 3C).

Mitochondrial velocity is also an essential parameter of mitochondrial motility and dynamics; the velocity of motile mitochondria was also measured from kymographs. Remarkably, the motile mitochondria in *Opa1*$^{+/-}$ RGC neurites presented an increased velocity (0.39 ± 0.024 µm/s) compared with the wild-type (0.24 ± 0.026 µm/s): the velocity was increased by approximately 0.15 µm/s ($P < 0.05$, see Fig. 3D). Moreover, mitochondrial movements presented a concomitant increase in contact rates between mitochondria in Opa1$^{+/-}$ RGCs (0.092 ± 0.0070 contacts/mitochondrion/rate) compared with the wild-type (0.050 ± 0.010 contacts/mitochondrion/rate, $P < 0.05$, see Fig. 3E). These results suggest that mitochondria in *Opa1*$^{+/-}$ RGCs display increased motility, with a larger number of motile mitochondria, increased movement velocity and a concomitant higher frequency of contacts in response to the Opa1 deficiency.

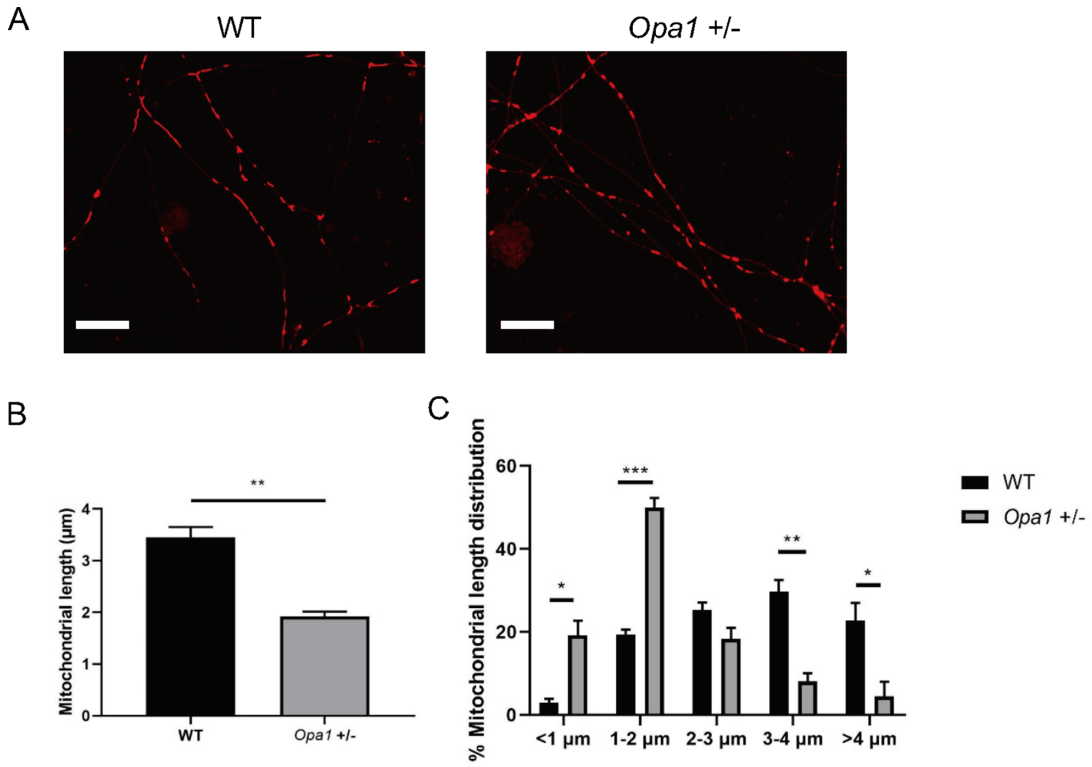

Figure 2. Opa1 deficiency results in decreased mitochondrial length in primary retinal ganglion cells (RGCs) from *Opa1*$^{+/-}$ mouse compared to wild-type. (**A**) The representative images with MitoTracker Red from wild-type and *Opa1*$^{+/-}$ RGCs cultures on the eighth day in vitro. (**B**) The comparison of mitochondrial length in μm. (C) The distribution of mitochondrial length between wild-type and *Opa1*$^{+/-}$ RGCs. The lengths of 658 mitochondria from wild-type RGC neurites and 812 mitochondria from *Opa1*$^{+/-}$ RGC neurites were calculated. The results are shown as means ± SEM, from three independent experiments. *$P < 0.05$, **$P < 0.01$, ***$P < 0.001$ vs. wild-type. Scale bar = 20 μm.

Opa1 Deficiency Leads to Impaired Mitochondrial Bioenergetics in Primary Mouse RGCs

To explore how Opa1 deficiency in the B6; C3-Opa1^{Q285STOP} mouse influences mitochondrial bioenergetics in mouse primary retinal ganglion cells, cellular OCRs were measured in real time using the Seahorse XF^{e} 96 Extracellular Flux Analyzer with sequential injection of mitochondrial respiration inhibitors. As shown in Figure 4B, Opa1 deficiency caused a significant decline in the basal respiration compared with the wild-type ($P < 0.05$) in the mouse primary retinal ganglion cells. The first compound injected in the assay was oligomycin, a complex V (ATP synthase) inhibitor, used to clarify the proportion of ATP-linked respiration in the basal respiration. The second injected compound was FCCP, an uncoupling agent for collapsing the proton gradient and disrupting the mitochondrial membrane potential, used to determine the maximal respiration. A combination treatment of antimycin A (complex III inhibitor) and rotenone (complex I inhibitor) was finally injected to shut down the whole mitochondrial respiration. A significant decline was observed in ATP-linked respiration, decreased by ~21.16 pmol/min per 10,000 cells ($P < 0.05$, see Fig. 4C), and maximal respiration, decreased by ~51.09 pmol/min per 10,000 cells ($P < 0.05$, see Fig. 4D), respectively. Spare respiratory capacity, an indicator of cellular fitness which illustrates the capability of each cell to respond to an energetic demand via oxidative phosphorylation is calculated by subtracting maximal OCR from the basal OCR. The reserve capacity of mitochondrial respiration was shown to be significantly lower in *Opa1*$^{+/-}$ retinal ganglion cells compared with the wild-type (decreased by ~28.65 pmol/min per 10,000 cells, $P < 0.05$, see Fig. 4E). Overall, these results from the OCR assay showed that Opa1 deficiency caused lower basal respiration, decreased ATP-linked oxygen consumption, diminished maximum value of oxidative phosphorylation, and depletion of the cellular capability for energy supply in mouse retinal ganglion cells.

Discussion

ADOA is an inherited optic neuropathy characterized by mitochondriopathy, which appears to result in selective RGC degeneration in the retina, followed by ascending optic atrophy. The exquisite vulnerability of RGCs to mitochondrial deficits caused by ADOA mutations may be associated with the acute energy demand along the neurites combined with their unique morphology.[8] Here we demonstrate for the first time that fragmented mitochondria caused by Opa1 deficiency showed an actively increased motility along RGC neurites in the presence of diminished mitochondrial bioenergetic function in RGCs isolated from B6; C3-*Opa1*^{Q285STOP} mouse model.

Mitochondrial morphology is the result of a balance between fusion and fission processes, and results in the existence of small fragments or elongated tubular structures based on the metabolic state of the cell. The defects in Opa1 in our primary RGCs firstly caused fragmentation of the tubular mitochondrial reticulum in RGCs, in which the

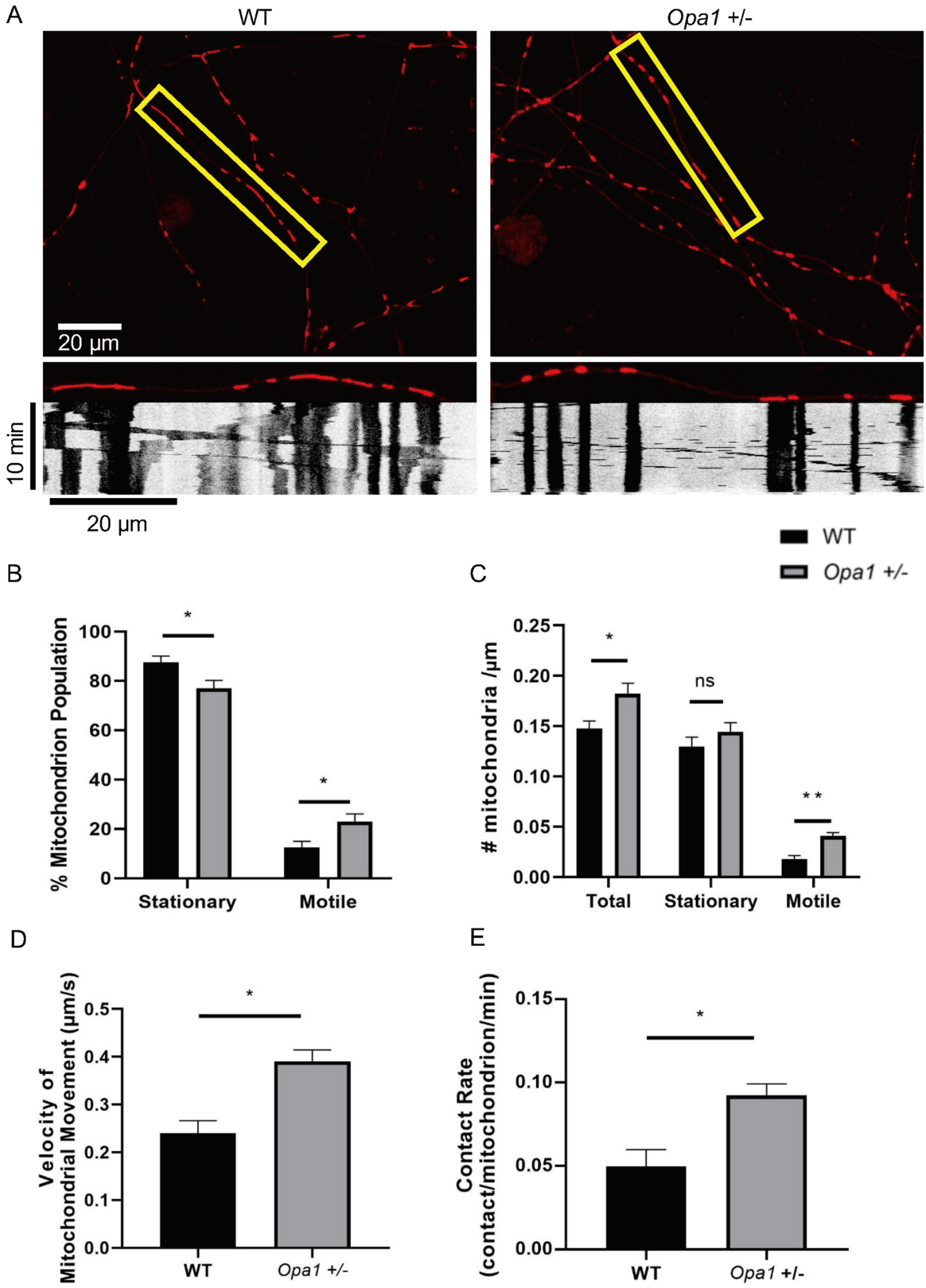

Figure 3. Opa1 deficiency results in increased mitochondrial motility in primary retinal ganglion cells (RGCs) from *Opa1*$^{+/-}$ mouse compared to wild-type. (**A**) Mitochondrial movement was visualized by MitoTracker Red and recorded by time-lapse imaging on the eighth day in vitro. The movements were traced manually from automatically generated kymographs using FIJI software. Three key parameters of mitochondrial motility were calculated: (**B**) distribution of the mitochondrion population classified as stationary and motile; (**C**) densities of mitochondria calculated as the number of mitochondria per neurite length; (**D**) velocities of mitochondrial movement; (**E**) the contact rate

calculated as the number of contacts between mitochondria divided by the total number of mitochondria per minute in each imaged region. In total 1280 mitochondria, from 91 wild-type RGC neurites and 1205 mitochondria, from 92 *Opa1*$^{+/-}$ RGC neurites were measured. The results are shown as means ± SEM, from three independent experiments. *$P < 0.05$, **$P < 0.01$ vs. wild-type. Scale bar = 20 µm.

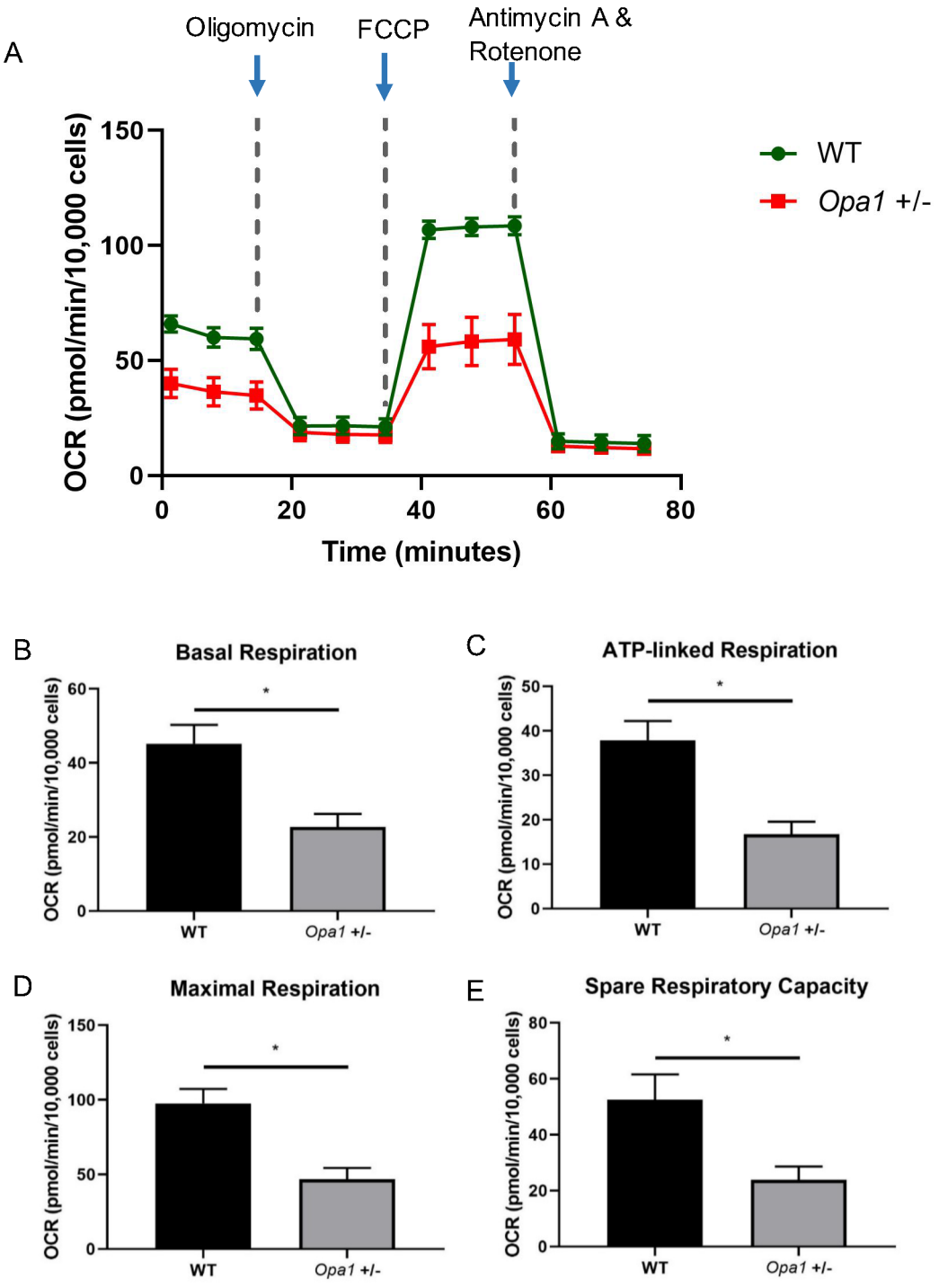

Figure 4. Comparative analysis of mitochondrial bioenergetics between wild-type and *Opa1*$^{+/-}$ mouse primary retinal ganglion cells. Cells were measured on the third day in vitro. (**A**) OCR profile plot. Oxygen consumption rate (OCR) was recorded by Seahorse Extracellular Flux Analyzer at baseline and after the sequential injections of oligomycin (1 µmol/L), FCCP (2.5 µmol/L), and a mixture of rotenone and antimycin (1 µmol/L). (**B**) Basal respiration, (**C**) ATP-linked respiration, (**D**) maximal respiration, (**E**) spare respiratory capacity was calculated. Data are shown as the mean ± SEM of three independent experiments, each with five replicates. *$P < 0.05$ vs. wild-type group.

lengths of mitochondria in *Opa1*$^{+/-}$ RGCs were decreased to nearly half of that in the wild-type. These results are consistent with the punctate pattern of mitochondria in mouse embryonic fibroblasts (MEFs) from *Opa1*^{Q285STOP} mouse model,[16] and in lymphoblastoid cell lines and fibroblasts derived from ADOA patients.[17–19] Mitochondria are actively transported along microtubule tracks from the soma to the RGC neurites, which is an energy-demanding process in mammals.[8] Interactions between polarized microtubules, motor proteins, adaptors that link motor proteins to mitochondria and anchors that arrest transport have been demonstrated to trigger the motility of mitochondria.[20] It has also been reported that the activation of the energy biosensor AMP-activated protein kinase (AMPK) contributes to the detection of the energy deprivation in neurons which contributes to the recruitment of mitochondria to the energy-deficient area.[21] The interplay in mitochondrial dynamics, including the morphology, motility and fusion-fission balance, are likely to be sophisticated and delicate. Previous studies demonstrated that augmented motility with a higher number of mitochondria in the neighborhood could increase the likelihood of contacts between individual mitochondrion, which was consequently associated with the probability of fusion process. Furthermore, increased fusion activity could then elongate the length of mitochondria in turn probably activating the machinery of fission process in order to inhibit a further elongation of mitochondrial length.[22,23] Additionally, it was shown that inhibited mitochondrial motility caused by nocodazol and vasopressin led to suppressed merging frequency in H9c2 cells.[24] In our study, Opa1 deficiency caused shortened length of mitochondrial structures, an augmented number of motile mitochondria, with higher moving speed and was also accompanied by increased contact frequency between mitochondria. It may be speculated that shortened mitochondria were stimulated to increase motility in an attempt to increase the possibility of fusion activity, which may be a response to rescue the mitochondrial phenotype in RGCs suffering from Opa1 deficiency.

Apart from the promotion of the fusion process, OPA1 also works as a master regulator of cristae structure and remodeling, independently of its role in fusion.[25,26] Since cristae are critical to the machinery of mitochondrial oxidative phosphorylation as the complexes of electron transport chain are located within the large surface area of the cristae, OPA1 therefore plays an essential role in regulating mitochondrial respiratory efficiency by directly changing the control of cristae widening or constriction.[27–29] Additionally, elongated mitochondria also presented higher activity of energy production because of the larger area of cristae, higher levels of dimers of the ATPase as well as the escape from autophagic degradation,[30] emphasizing the vital character of OPA1 in modulating mitochondrial bioenergetics and cell metabolism. However, the indicators of mitochondrial bioenergetics in samples from patients with ADOA mutations has revealed some controversial and sometimes conflicting results. Defective oxidative phosphorylation with remarkably reduced mitochondrial adenosine triphosphate production rate was observed in calf muscle in vivo from six patients,[31] consistent with the impaired ATP synthesis driven by complex I substrates in skin fibroblasts derived from ADOA patients,[32] and the reduced oxygen consumption as well as dysfunctional bioenergetics in lymphoblastoid cells obtained from four ADOA families.[19] In contrast, no alterations in mitochondrial oxidative phosphorylation were observed in lymphoblastoid cells lines and fibroblasts derived from patients,[33] which were not associated with the fragmented morphology.[34] These conflicting results may be due to the distinct effects of *OPA1* mutations in different cell types and might be associated with different bioenergetic profiles seen with different *OPA1* mutations. Because the RGC is a cell type highly vulnerable to metabolic disturbances and is exquisitely affected in patients with ADOA, it is conceivable that the results of our mitochondrial measurements might be different in RGCs from other cell types. According to our study, mitochondrial bioenergetics in panned RGCs from the B6; C3-*Opa1*^{Q285STOP} mouse model revealed an impaired mitochondrial respiratory function with diminished reserve capacity in RGCs with Opa1 deficiency. Therefore, we propose, evidence that mitochondrial bioenergetics and energy production can be disrupted in RGCs as a result of OPA1 deficiency.

The critical role of mitochondria is central not only in ADOA but also another classical optic neuropathy—Leber hereditary optic neuropathy—and even in some neurodegenerative diseases such as Alzheimer's, Parkinson's and Huntington's diseases in the central nervous system (CNS).[35] In ADOA, in addition to the clinical visual loss caused by the degeneration of optic nerves projected from about 1.2 million RGCs in the retina, some patients display a "plus" phenotypes in a wider range of tissues including CNS and brain, indicating a broader link between mitochondrial dysfunction caused by OPA1 deficit and neurodegeneration within the CNS.[36] OPA1 exerts critical roles in mitochondrial energy production through two independent pathways. First, OPA1 protein directly affects cristae modeling by OPA1 to help regulate the mitochondrial energy production through oxidative phosphorylation. OPA1 also helps equilibrate the mitochondrial dynamic balance and enhances the fusion process, so that the elongated mitochondria with a larger area of cristae are more likely to consist of higher levels of dimers of the ATPase and escape from autophagic degradation, which also enhances mitochondrial bioenergetics. Thus in ADOA, we speculated that OPA1 deficit could cause impaired mitochondrial bioenergetics through fragmentation of mitochondrial morphology or direct damage of cristae structure. Surprisingly, with a larger number of mitochondria detected in the neurites of RGCs with higher motility, there would be higher probability of mitochondrial contact. Because fusion activity could only occur when two mitochondria meet, the higher contact rate can then increase the possibility of fusion. Although only less than 10% contacts could result in fusion reported in cortical neurons,[22] the mitochondria with increased contact rates can also be benefit from mitochondrial "kiss-and-run" interplays—transient fusions that could also be an alternative support for mitochondrial metabolism.[24] In this pathway the mitochondrial bioenergetics can be also promoted consequently. Thus we infer that the activated motility under OPA1 deficit in RGC neurites could be a spontaneous compensation in an attempt to rescue the impaired fusion and fission balance, as well as mitochondrial bioenergetics (Fig. 5).

Previous research has demonstrated that about a third of mitochondria are highly mobile before any branching patterns in dendrites are established. Mitochondria become largely stationary as they reach their positions at the synapses and branch points where energy is needed in mature RGC dendrites.[37] Takihara et al.[38] developed minimally invasive intravital multiphoton imaging to record the

Investigative Ophthalmology & Visual Science

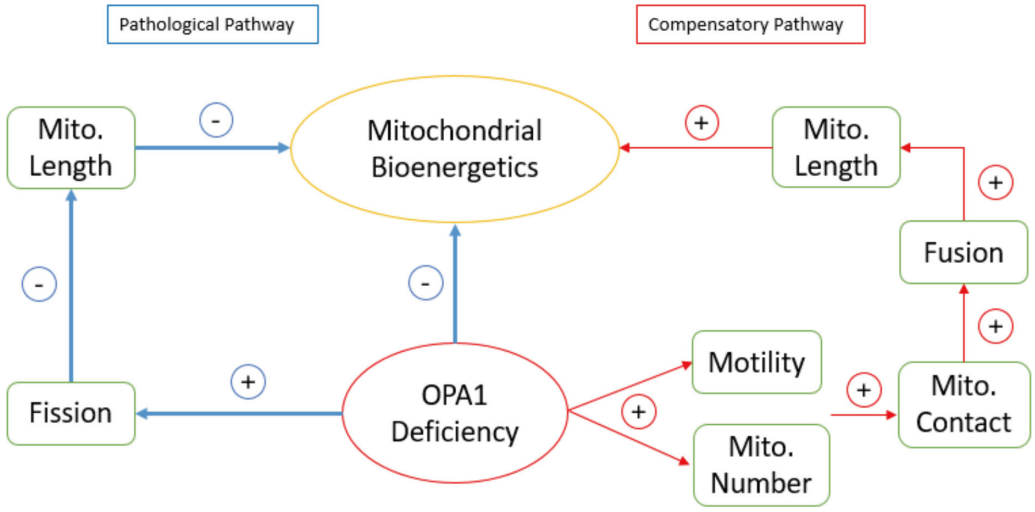

Figure 5. Summarized hypothesis of the pathological mechanisms of ADOA and the spontaneous compensatory pathway through mitochondrial motility activation.

transportation of mitochondria in a single axon of RGCs in vivo and illustrated the dynamics in axonal transport of mitochondria during aging as well as the disturbances of mitochondrial transport in a mouse glaucoma model. Previous studies also demonstrated that mitochondria were prominent in growth cones and preferentially recruited into distal axons where actively extending through the AMP-activated protein kinase (AMPK) energy-sensing pathway.[39–41] Specifically, Steketee et al.[42] demonstrated the critical role of mitochondrial fission in normal growth cone dynamics and axon extension by acutely inhibiting Drp1 function using mDivi-1 in rat retinal ganglion cell axons. Moreover, numerous intrinsic and extrinsic factors that regulate the axonal growth also directly or indirectly effect the mitochondrial dynamics and function such as BDNF,[43] NGF,[44] PTEN,[45] and Nogo[46,47] in the CNS. Notably, Kreymerman et al.[48] found a novel mitochondrial fission protein, MTP18, that could regulate the mitochondrial size and also have a role in modulating neurite outgrowth in RGCs during development and injury conditions. Additionally, melanopsin-containing RGCs (mRGCs), a special subset of RGCs constituting only 1% of the RGC population in humans, were reported to be resistant to mitochondrial dysfunction and maintain the non-image-forming light driven functions[49,50] independently from melanopsin expression.[51] The large cellular size of mRGCs with a high cellular content of mitochondria might be the possible factors protecting mRGCs from mitochondrial dysfunctions.[49,52] Unlike primary cortical neurons cultured in vitro from fetal rodents which can establish synapse formation to mature status resembling that in the cerebral cortex in vivo,[53] purified RGCs cultured in vitro are unable to effectively form synapses without soluble astrocyte-derived signals.[54] Based on the findings in our current study from RGCs before the completion of synaptogenesis, we hypothesize that the increased motility of mitochondria could also possibly occur in mature RGCs with OPA1 deficit compared to normal RGCs in vivo. The generation of physiological relevant models, such as differentiated RGCs from induced pluripotent stem cells regenerated from patients' somatic cells, may assist in answering future questions.

Taken together, our results suggest that Opa1 haploinsufficiency leads to significant fragmentation of mitochondrial morphology, activation of mitochondrial motility and impaired respiratory function in retinal ganglion cells from the B6; C3-*Opa1*^{Q285STOP} mouse model. The increased motility of mitochondria is hypothesized to be a spontaneous compensatory response which promotes fusion activity and facilitates energy production. More in-depth studies are required to investigate the interplay between mitochondrial motility and bioenergetics and the precise mechanisms underlying the stimulated mitochondrial motility caused by Opa1 deficiency, which could be a new target for therapeutic intervention.

Acknowledgments

Supported by China Scholarship Council (201706100202).

Disclosure: **S. Sun**, None; **I. Erchova**, None; **F. Sengpiel**, None; **M. Votruba**, None

References

1. Yu-Wai-Man P, Bailie M, Atawan A, Chinnery PF, Griffiths PG. Pattern of retinal ganglion cell loss in dominant optic atrophy due to OPA1 mutations. *Eye (Lond)*. 2011;25:596–602.
2. Puomila A, Huoponen K, Mantyjarvi M, et al. Dominant optic atrophy: correlation between clinical and molecular genetic studies. *Acta Ophthalmol Scand*. 2005;83:337–346.
3. Chun BY, Rizzo JF, 3rd. Dominant optic atrophy: updates on the pathophysiology and clinical manifestations of the optic atrophy 1 mutation. *Curr Opin Ophthalmol*. 2016;27:475–480.
4. Chun BY, Rizzo JF, 3rd. Dominant Optic Atrophy and Leber's Hereditary Optic Neuropathy: Update on Clinical Features and Current Therapeutic Approaches. *Semin Pediatr Neurol*. 2017;24:129–134.
5. Ferre M, Bonneau D, Milea D, et al. Molecular screening of 980 cases of suspected hereditary optic neuropathy with a report on 77 novel OPA1 mutations. *Hum Mutat*. 2009;30:E692–E705.
6. Alavi MV, Fuhrmann N. Dominant optic atrophy, OPA1, and mitochondrial quality control: understanding mitochondrial network dynamics. *Mol Neurodegener*. 2013;8:32.

7. Kjer P, Jensen OA, Klinken L. Histopathology of eye, optic nerve and brain in a case of dominant optic atrophy. *Acta Ophthalmol (Copenh)*. 1983;61:300–312.
8. Ito YA, Di Polo A. Mitochondrial dynamics, transport, and quality control: A bottleneck for retinal ganglion cell viability in optic neuropathies. *Mitochondrion*. 2017;36:186–192.
9. Davies VJ, Hollins AJ, Piechota MJ, et al. Opa1 deficiency in a mouse model of autosomal dominant optic atrophy impairs mitochondrial morphology, optic nerve structure and visual function. *Hum Mol Genet*. 2007;16:1307–1318.
10. Winzeler A, Wang JT. Purification and culture of retinal ganglion cells from rodents. *Cold Spring Harb Protoc*. 2013;2013:643–652.
11. Barres BA, Silverstein BE, Corey DP, Chun LL.. Immunological, morphological, and electrophysiological variation among retinal ganglion cells purified by panning. *Neuron*. 1988;1:791–803.
12. Hu X, Dai Y, Sun X. Parkin overexpression protects retinal ganglion cells against glutamate excitotoxicity. *Mol Vis*. 2017;23:447–456.
13. Gao F, Li T, Hu J, Zhou X, Wu J, Wu Q. Comparative analysis of three purification protocols for retinal ganglion cells from rat. *Mol Vis*. 2016;22:387–400.
14. Kamei S, Chen-Kuo-Chang M, Cazevieille C, et al. Expression of the Opa1 mitochondrial protein in retinal ganglion cells: its downregulation causes aggregation of the mitochondrial network. *Invest Ophthalmol Vis Sci*. 2005;46:4288–4294.
15. Neumann S, Chassefeyre R, Campbell GE, Encalada SE. KymoAnalyzer: a software tool for the quantitative analysis of intracellular transport in neurons. *Traffic*. 2017;18:71–88.
16. Kushnareva Y, Seong Y, Andreyev AY, et al. Mitochondrial dysfunction in an Opa1(Q285STOP) mouse model of dominant optic atrophy results from Opa1 haploinsufficiency. *Cell Death Dis*. 2016;7:e2309.
17. Zhang J, Liu X, Liang X, et al. A novel ADOA-associated OPA1 mutation alters the mitochondrial function, membrane potential, ROS production and apoptosis. *Sci Rep*. 2017;7:5704.
18. Liao C, Ashley N, Diot A, et al. Dysregulated mitophagy and mitochondrial organization in optic atrophy due to OPA1 mutations. *Neurology*. 2017;88:131–142.
19. Kao SH, Yen MY, Wang AG, Yeh YL, Lin AL. Changes in Mitochondrial Morphology and Bioenergetics in Human Lymphoblastoid Cells With Four Novel OPA1 Mutations. *Invest Ophthalmol Vis Sci*. 2015;56:2269–2278.
20. Barnhart EL. Mechanics of mitochondrial motility in neurons. *Curr Opin Cell Biol*. 2016;38:90–99.
21. Tao K, Matsuki N, Koyama R. AMP-activated protein kinase mediates activity-dependent axon branching by recruiting mitochondria to axon. *Dev Neurobiol*. 2014;74:557–573.
22. Cagalinec M, Safiulina D, Liiv M, et al. Principles of the mitochondrial fusion and fission cycle in neurons. *J Cell Sci*. 2013;126:2187–2197.
23. Twig G, Liu X, Liesa M, et al. Biophysical properties of mitochondrial fusion events in pancreatic beta-cells and cardiac cells unravel potential control mechanisms of its selectivity. *Am J Physiol Cell Physiol*. 2010;299:C477–C487.
24. Liu X, Weaver D, Shirihai O, Hajnoczky G. Mitochondrial 'kiss-and-run': interplay between mitochondrial motility and fusion-fission dynamics. *EMBO J*. 2009;28:3074–3089.
25. Meeusen S, DeVay R, Block J, et al. Mitochondrial inner-membrane fusion and crista maintenance requires the dynamin-related GTPase Mgm1. *Cell*. 2006;127:383–395.
26. Cogliati S, Frezza C, Soriano ME, et al. Mitochondrial cristae shape determines respiratory chain supercomplexes assembly and respiratory efficiency. *Cell*. 2013;155:160–171.
27. Frezza C, Cipolat S, Martins de Brito O, et al. OPA1 controls apoptotic cristae remodeling independently from mitochondrial fusion. *Cell*. 2006;126:177–189.
28. Pernas L, Scorrano L. Mito-Morphosis: Mitochondrial Fusion, Fission, and Cristae Remodeling as Key Mediators of Cellular Function. *Annu Rev Physiol*. 2016;78:505–531.
29. Wollweber F, von der Malsburg K, van der Laan M. Mitochondrial contact site and cristae organizing system: A central player in membrane shaping and crosstalk. *Biochim Biophys Acta Mol Cell Res*. 2017;1864:1481–1489.
30. Gomes LC, Di Benedetto G, Scorrano L. During autophagy mitochondria elongate, are spared from degradation and sustain cell viability. *Nat Cell Biol*. 2011;13:589–598.
31. Lodi R, Tonon C, Valentino ML, et al. Deficit of in vivo mitochondrial ATP production in OPA1-related dominant optic atrophy. *Ann Neurol*. 2004;56:719–723.
32. Zanna C, Ghelli A, Porcelli AM, et al. OPA1 mutations associated with dominant optic atrophy impair oxidative phosphorylation and mitochondrial fusion. *Brain*. 2008;131:352–367.
33. Mayorov VI, Lowrey AJ, Biousse V, Newman NJ, Cline SD, Brown MD. Mitochondrial oxidative phosphorylation in autosomal dominant optic atrophy. *BMC Biochem*. 2008;9:22.
34. Spinazzi M, Cazzola S, Bortolozzi M, et al. A novel deletion in the GTPase domain of OPA1 causes defects in mitochondrial morphology and distribution, but not in function. *Hum Mol Genet*. 2008;17:3291–3302.
35. Yu-Wai-Man P, Newman NJ. Inherited eye-related disorders due to mitochondrial dysfunction. *Hum Mol Genet*. 2017;26:R12–R20.
36. Yu-Wai-Man P, Votruba M, Burte F, La Morgia C, Barboni P, Carelli V. A neurodegenerative perspective on mitochondrial optic neuropathies. *Acta Neuropathol*. 2016;132:789–806.
37. Faits MC, Zhang C, Soto F, Kerschensteiner D. Dendritic mitochondria reach stable positions during circuit development. *Elife*. 2016;5:e11583.
38. Takihara Y, Inatani M, Eto K, et al. In vivo imaging of axonal transport of mitochondria in the diseased and aged mammalian CNS. *Proc Natl Acad Sci USA*. 2015;112:10515–10520.
39. Morris RL, Hollenbeck PJ. The regulation of bidirectional mitochondrial transport is coordinated with axonal outgrowth. *J Cell Sci*. 1993;104(Pt 3):917–927.
40. Ruthel G, Hollenbeck PJ. Response of mitochondrial traffic to axon determination and differential branch growth. *J Neurosci*. 2003;23:8618–8624.
41. Cunniff B, McKenzie AJ, Heintz NH, Howe AK. AMPK activity regulates trafficking of mitochondria to the leading edge during cell migration and matrix invasion. *Mol Biol Cell*. 2016;27:2662–2674.
42. Steketee MB, Moysidis SN, Weinstein JE, et al. Mitochondrial dynamics regulate growth cone motility, guidance, and neurite growth rate in perinatal retinal ganglion cells in vitro. *Invest Ophthalmol Vis Sci*. 2012;53:7402–7411.
43. Markham A, Cameron I, Franklin P, Spedding M. BDNF increases rat brain mitochondrial respiratory coupling at complex I, but not complex II. *Eur J Neurosci*. 2004;20:1189–1196.
44. Chada SR, Hollenbeck PJ. Nerve growth factor signaling regulates motility and docking of axonal mitochondria. *Curr Biol*. 2004;14:1272–1276.
45. Park KK, Liu K, Hu Y, et al. Promoting axon regeneration in the adult CNS by modulation of the PTEN/mTOR pathway. *Science*. 2008;322:963–966.
46. Goldberg JL, Barres BA. Nogo in nerve regeneration. *Nature*. 2000;403:369–370.

Investigative Ophthalmology & Visual Science

47. Hu WH, Hausmann ON, Yan MS, Walters WM, Wong PK, Bethea JR. Identification and characterization of a novel Nogo-interacting mitochondrial protein (NIMP). *J Neurochem*. 2002;81:36–45.
48. Kreymerman A, Buickians DN, Nahmou MM, et al. MTP18 is a Novel Regulator of Mitochondrial Fission in CNS Neuron Development, Axonal Growth, and Injury Responses. *Sci Rep*. 2019;9:10669.
49. La Morgia C, Ross-Cisneros FN, Sadun AA, et al. Melanopsin retinal ganglion cells are resistant to neurodegeneration in mitochondrial optic neuropathies. *Brain*. 2010;133:2426–2438.
50. Perganta G, Barnard AR, Katti C, et al. Non-image-forming light driven functions are preserved in a mouse model of autosomal dominant optic atrophy. *PLoS One*. 2013;8:e56350.
51. Gonzalez-Menendez I, Reinhard K, Tolivia J, Wissinger B, Munch TA. Influence of Opa1 Mutation on Survival and Function of Retinal Ganglion Cells. *Invest Ophthalmol Vis Sci*. 2015;56:4835–4845.
52. Georg B, Ghelli A, Giordano C, et al. Melanopsin-expressing retinal ganglion cells are resistant to cell injury, but not always. *Mitochondrion*. 2017;36:77–84.
53. Ichikawa M, Muramoto K, Kobayashi K, Kawahara M, Kuroda Y. Formation and maturation of synapses in primary cultures of rat cerebral cortical cells: an electron microscopic study. *Neurosci Res*. 1993;16:95–103.
54. Ullian EM, Sapperstein SK, Christopherson KS, Barres BA. Control of synapse number by glia. *Science*. 2001;291:657–661.

Investigative Ophthalmology & Visual Science